LEGIBILITY NOTICE

A major purpose of the Technical Information Center is to provide the broadest dissemination possible of information contained in DOE's Research and Development Reports to business, industry, the academic community, and federal, state and local governments.

Although a small portion of this report is not reproducible, it is being made available to expedite the availability of information on the research discussed herein.

1

LA-UR -90-2131

LA-UR--90-2131

DE90 013158

Los Alamos National Laboratory is operated by the University of California for the United States Department of Energy under contract W-7405-ENG-36

TITLE On the Nature of the Plasma Sheet Boundary Layer

AUTHOR(S) E.W. Hones, Jr.

SUBMITTED TO XXVIII COSPAR Plenary Meeting, The Hague, The Netherlands, 25 June - 6 July 1990

Los Alamos

Los Alamos National Laboratory
Los Alamos, New Mexico 87545

ON THE NATURE OF THE PLASMA SHEET BOUNDARY LAYER

E. W. Hones, Jr.

*Mission Research Corporation**
Los Alamos, NM 87544, U.S.A.

ABSTRACT

The regions of the plasma sheet adjacent to the north and south lobes of the magnetotail have been described by many experimenters as locations of beams of energetic ions and fast-moving plasma directed primarily earthward and tailward along magnetic field lines. Measurements taken as satellites passed through one or the other of these boundary layers have frequently revealed near-earth mirroring of ions and a vertical segregation of velocities of both earthward-moving and mirroring ions with the fastest ions being found nearest the lobe-plasma sheet interface. These are features expected for particles from a distant tail source $\overline{E} \times \overline{B}$ drifting in a dawn-to-dusk electric field and are consistent with the source being a magnetic reconnection region. The plasma sheet boundary layers are thus understood as separatrix layers, bounded at their lobeward surfaces by the separatrices from the distant neutral line. This paper will review the observations that support this interpretation.

INTRODUCTION

In the complex environment of magnetized plasma that comprises the Earth's magnetosphere and that arises from the interaction of the magnetized solar wind with the earth's magnetic field, important boundaries exist at surfaces across which the topology of the magnetic field changes. The importance of these boundaries arises, in part, because they separate domains of plasmas having different origins and characteristics. But their greatest importance stems from the fact that they are sites where magnetic reconnection occurs, when conditions are appropriate, determining the coupling between the solar wind and magnetosphere domains and thus establishing the dynamic behavior of the whole magnetosphere. The primary such boundary is, of course, the magnetopause where the solar wind (magnetosheath) and magnetosphere plasma domains meet. When the magnetic field directions across this boundary are opposed (i.e., when the interplanetary field is southward) magnetic reconnection occurs, resulting in the delivery of a larger amount of solar

* Also a Guest Scientist at the Los Alamos National Laboratory

wind energy to the magnetosphere. In the magnetotail the magnetic fields in the north and south lobes are always opposed and magnetic reconnection between these two domains proceeds all the time, creating the plasma sheet and determining how, and at what rate, the magnetosphere will dispose of the energy it acquires from the solar wind.

Because of the magnetic reconnection that occurs in the magnetotail there are always at least three different magnetic topologies there and, when substorms occur there is a fourth topology in addition to these. Figure 1 portrays four different states of the magnetotail. Figure 1A represents the quiescent state having a single magnetic neutral line (reconnection site) located some 100 R_E downtail from the earth. Earthward of the neutral line the plasma sheet contains closed field lines, both ends attached to the earth. The north and south tail lobes contain open field lines, one end attached to earth, the other end extending into the solar wind far downtail. Tailward of the neutral line the plasma sheet contains interplanetary field lines, both ends extending into the solar wind, with no attachment to the earth.

Figure 1B shows the situation shortly after the onset of a magnetospheric substorm. Closed lines of the plasma sheet have been severed by magnetic reconnection at a near-earth "substorm neutral line" that formed some 10-20 R_E tailward of earth and thus a fourth magnetic topology has been created - a plasmoid - closed magnetic loops that connect neither with the earth nor with the solar wind. A region of closed field lines, tied to earth, still exists but is much reduced in size by the magnetic reconnection at the substorm neutral line.

Figure 1C shows the situation some half-hour after substorm onset. The plasmoid has moved perhaps 100 R_E downtail while the substorm neutral line remains stationary near the location of its original formation. After the plasmoid was formed and freed from earth by severance of the last closed field line of the pre-substorm plasma sheet, lobe field lines began to reconnect at the substorm neutral line, creating new interplanetary field lines which enshroud the retreating plasmoid, collapsing tailward behind it. They tend to pile up behind the plasmoid, creating a thickening region behind it called the post-plasmoid plasma sheet (PPPS).

Figure 1D shows the situation perhaps one hour after substorm onset. The plasmoid has retreated downtail to the right and the substorm neutral line has begun to retreat tailward where it will eventually stop at ~100 R_E. The region of closed field lines and earthward jetting plasma created earthward of it will restore the plasma sheet to its pre-substorm configuration.

It is to be noted that interfaces exist between the plasma sheet and the north and south lobes over the full extent of the plasma sheet under all four conditions. These surfaces or "separatrices" lie, in some places, between lobe (open) field lines and closed field lines and, in other places, between lobe field lines and interplanetary field lines. The top panel of Fig. 1 portrays the dawn-to-dusk electric field and the resulting equatorward $\overline{E} \times \overline{B}$ drift (convection) that causes the reconnection to proceed at the neutral lines (x-lines). Lobe field lines, reconnected at the neutral line, snap earthward and tailward joining the regions of closed and interplanetary field lines. Ions and electrons are accelerated, some to hundreds of keV, in the near vicinity of the x-line and escape earthward and tailward, moving with speeds characteristic of their energies along the newly created closed and interplanetary field lines. As they proceed away from the neutral line, they continue to drift, all at the same $\overline{E} \times \overline{B}$ speed, toward the equator. Thus layers of moving particles are formed at the north and south plasma sheet-lobe interfaces with the fastest particles moving on field lines nearest the separatrices. (Particles with infinite velocity would move on the separatrices; 100 keV electrons with velocity ~2 × 10^5 km/sec, would be on field lines lying ~150 km equatorward of the separatrices when they have gone 100 R_E from the x-line).

This, then, is the origin of the plasma sheet boundary layer, the region at the north and south boundaries of the plasma sheet characterized by particle populations jetting along the magnetic field lines. This region, which is in essence the lobe-plasma sheet "separatrix layer," has been of great interest to magnetospheric scientists for many years and has received added attention in the last five years because of a role that has been claimed for it /1/ in creating certain plasma and particle flow signatures that have been otherwise interpreted as indications of magnetic reconnection at the near-earth neutral line during substorms.

This paper describes several sets of observations, in both the near and far magnetotail, that have established the identity of the plasma sheet boundary layer as the separatrix layer associated with the lobe-plasma sheet interface.

NEAR-TAIL OBSERVATIONS OF THE BOUNDARY LAYER

It is important to recall in discussing observations of the boundary layer either in the near tail or the far tail that satellite crossings of the layer are almost never due to the motions of the satellite but to motions (or expansions or contractions) of the plasma sheet itself. Furthermore, the largest, most rapid motions of the boundary and the most dramatic jetting of particles are those associated with the plasma sheet's expansion (i.e., with the neutral line's retreat) during substorm recoveries. Thus, much of the literature published about the boundary layer relates to its observation during these substorm recovery episodes.

The importance of these episodes in establishing the average plasma flow behavior in the boundary layer is nicely illustrated by Fig. 2, which shows the average occurrence rate of plasma ion flows exceeding 300 km/sec versus position in the plasma sheet edge and the boundary layer. The frequency of occurrence is by far the greatest during inward crossings beyond X_{GSM} = -14 R_E. Most of such crossings are related to substorm recoveries.

The structuring of plasma flow in the near-earth plasma sheet boundary layer and the association of this region with the plasma sheet-lobe separatrix became clearly recognized through the study of ISEE 1 and 2 plasma measurements by Takahashi and Hones /2/. Figure 3 shows data they examined from ISEE 1 orbiting high above the neutral sheet in the near-midnight sector earthward of $X_{SM} = -14$ R_E. This was an interval of quite strong geomagnetic activity, but other orbits they analyzed occurred during both quiet and more active times. Early identifications of the plasma sheet boundary layer were made principally using the feature of rapid plasma flow or ion jetting as the identifier (e.g., Eastman *et al.* /1/). But this became clearly inappropriate when features of the boundary layer itself (including the plasma flow features) were to be studied. Thus Takahashi and Hones related ion pressure to plasma bulk velocity and found that the fast flow region was also one of ion pressure significantly reduced from that of the plasma sheet. This is illustrated in Fig. 4. An analogous identifier of the boundary layer lies in the absence or presence of photoelectrons around the satellite and thus spacecraft charging /3/. A spacecraft is charged only to a very low potential in the plasma sheet but becomes more highly charged in the more tenuous plasma of the boundary layer. The appearance of photoelectrons is a very sensitive indicator of the increased spacecraft potential and thus of the reduced plasma density.

The third panel of Fig. 3 shows intervals of fast (mostly earthward) ion bulk flow (the first moment of the ion velocity distribution function) that accompany reductions of plasma pressure. The period 2000-2030 UT, which contains two prominent such intervals, is shown expanded in Fig. 5. The bottom panel of Fig. 5 is a representation of a cut of the velocity distribution function along the sunward–antisunward (X_{SM}) axis. Some important points that can be discerned in Fig. 5 are:

a) Upon each appearance of plasma the earthward-going ions are seen first.

b) The fastest ions appear before slower ions. This is true for tailward-going ions as well as for earthward-going ions.

c) Fast (earthward) bulk flows are recorded when the earthward-going ion population exceeds those going tailward. (Note that a period of weak tailward bulk flow occurs at 2012-2013 resulting from an excess of tailward-going ions.)

Examination of the full distribution (not just the X_{SM} components) shows that it consists largely of just the x-aligned components. The delayed tailward-going portion comprises ions that have first gone earthward, have been reflected near the earth, and are proceeding tailward. Detailed examination of the distribution functions at these times shows that the tailward-going ions are faster than the earthward-going ions measured at the same instant, a phenomenon that was discovered by Forbes *et al.* /4/ and recognized by them as signifying reflected ions in an equatorward $\overline{E} \times \overline{B}$ drifting plasma. Such behavior is consistent with magnetic reconnection models (e.g., /5/) in which the particles accelerated to highest energy in the cross-tail electric field are those traversing the tail nearest the x-line; the reflected ions at a given location must, by geometrical necessity, have been accelerated nearer to the x-line than the earthward-going ions at the same point. The counter-streaming ions no doubt have a tendency to become thermalized through instabilities. Yet the lower panel of Fig. 3 shows that counter-streaming ion beams were seen for long periods following plasma sheet expansions over ISEE, suggesting their occurrences at substantial depths within the plasma sheet.

Takahashi and Hones /[illegible]/ examined all the transitions (inward and outward) between the plasma sheet and the lobe shown in Fig. 3 to determine the direction (earthward or tailward) of the very first (or the very last) ions detected. Out of 20 transitions (10 inward and 10 outward), 16 exhibited earthward streaming ions at the very edge of the plasma sheet. Only one case exhibited tailward streaming ions there. The remaining three exhibited counter-streaming ions of comparable intensities. The uniformity of these results, i.e., the constancy of the velocity structure of the beams in the boundary layer, regardless of its up or down motion is remarkable. Recall that it is not known what caused these up and down motions that resulted in the satellite's entries into and exits from the plasma sheet in this study. But their influence is evidently secondary to the process that defines the plasma structure at the edge of the plasma sheet.

Magnetic reconnection has been defined as the process whereby plasma flows across a surface that separates regions containing topologically different magnetic field lines /6/. The observations of Takahashi and Hones /2/ constitute compelling evidence that just such plasma flow must be occurring in the magnetotail. That is, they reveal the various components of the plasma sheet plasma, segregated by their linear velocities, convecting equatorward away from the lobe-plasma sheet separatrix after having, presumably, crossed that surface. The work strongly supports the view that the plasma sheet threaded by closed field lines is maintained by magnetic reconnection at a tailward neutral line and the resultant transport and energization of lobe plasma entering across the separatrix.

FAR-TAIL OBSERVATIONS OF THE BOUNDARY LAYER

One of the most remarkable observations made by the ISEE 3 satellite when it was taken from its orbit of the sunward Lagrangian point, L_1, in the solar wind to traverse the magnetotail in 1983 was that of plasmoids, created by substorms at earth, speeding tailward along the tail's midplane (as illustrated in Fig. 1) /7/. One of the features that was instrumental in providing recognition of the plasmoids and in understanding their true nature was the observation of segregated velocities of tailward-streaming particles in a magnetic field layer that enshrouded the plasmoids /8/ and that was quickly recognized as a separatrix layer just such as we have been discussing above /7/. Scholer *et al.* /8/ studied energetic particle bursts measured by ISEE 3 in the magnetotail ~ 220 R_E from earth. Data from one of these events are shown in Figures 6a and 6b and illustrate the following description. At the beginning of the bursts they first observed tailward-streaming electrons at an energy of 75–115 keV. These were followed after several minutes by anisotropic protons. The protons exhibited an energy dispersion with higher energy protons ($\sim$ 120 keV) appearing before lower energy ($\sim$ 32 keV) protons. The streaming electron distributions became (after $\sim$ 10 minutes) isotropic. An interpretation of the data in Figures 6a and 6b together with simultaneous magnetic field and plasma data is illustrated in Figure 7. The tailward streaming electrons detected starting at 0305 UT very closely marked ISEE 3's passage (A) from open field lines of the south lobe onto interplanetary field lines, newly created by reconnection of lobe field lines near the earth. Note that 200 keV electrons take only 7 seconds to travel from the Earth to ISEE 3. The slower-moving tailward-streaming ions indicated the satellite's passage deeper into the separatrix layer. The isotropization of the electrons and the broadening of the ion distributions at $\sim 0317-0319$ UT marked ISEE 3's passage (B) into the closed-loop structure of the plasmoid itself. Other data (not shown here) indicate that ISEE 2 exited briefly from the closed loop structure (C) and finally left it (D) returning thereafter to the south lobe.

Richardson and Cowley/10/ made detailed analyses of many energetic (> 35 keV) ion bursts (plasmoid passages) observed by ISEE 3 in the magnetotail $\sim$ 220 R_E from earth. They found that the bursts can usually be divided into four distinct phases: (a) strongly tailward streaming ions observed in lobe-like magnetic field for a few minutes prior to plasmoid entry; (b) the plasmoid interval, when the energetic ions have a broader tailward angular distribution arising from convection with the plasmoid; (3) the "post-plasmoid" plasma sheet (PPPS), where more strongly tailward streaming ions are observed in the plasma sheet on (interplanetary) field lines disconnected from the earth at the substorm neutral line; and (4) a strongly tailward streaming ion population extending into lobe-like magnetic field for a few minutes after exit from the PPPS. Concerning the layers of streaming ions observed on lobe-like field lines at the leading and trailing edges of these bursts (plasmoid encounters) they found a clear dawn-to-dusk gradient anisotropy and normal velocity dispersion (fastest particles encountered first) at the leading edge of the bursts, and the same gradient anisotropy with "inverse" velocity dispersion (fastest particles encountered last) at the trailing edge. They were also able to conclude that the ion onset at the leading edge is due to a layer of energetic ions being swept outward from the tail center plane by the approaching plasmoid; later, as the PPPS recedes down-tail, this ion layer is again observed, now with inverse dispersion. The line A-B-C-D in panel C of Figure 1 depicts ISEE 3's path through a passing plasmoid. Sections A-B and C-D of this path lie in the layers of streaming particles whose characteristics were described by Richardson and Cowley. The particle characteristics found there, tailward of the neutral line, are completely analogous to those found by Takahashi and Hones earthward of the neutral line and identify that region also as the separatrix layer.

CONCLUSIONS

The work that has been reviewed here is a small part of the extensive body of research and observations that have been reported in the literature regarding the boundary regions of the plasma sheet. But it is an extremely important part in that it addresses and reveals the characteristics that are essential in understanding the origin and true nature of the plasma sheet boundary layer. The work emphatically demonstrates features of plasma acceleration and convection, both near the earth and in the far tail, that can be understood as those theoretically expected at, and just equatorward of, the separatrix in a reconnecting magnetotail configuration. It demonstrates that the plasma sheet boundary layer is, in fact, the lobe-plasma sheet separatrix layer.

Acknowledgments. This work was done under the auspices of the U.S. Department of Energy.

REFERENCES

1. T. E. Eastman, L. A. Frank, W. K. Peterson, and W. Lennartsson, *J. Geophys. Res.* **89**, 1553 (1984).

2. K. Takahashi and E. W. Hones, Jr., *J. Geophys. Res.* **93**, 8558 (1988).

3. W. Baumjohann, G. Paschmann, N. Sckopke, C. A. Cattell, and C. W. Carlson, *J. Geophys. Res.* **93**, 11507 (1988).

4. T. G. Forbes, E. W. Hones, Jr., S. J. Bame, J. R. Asbridge, G. Paschmann, N. Sckopke, and C. T. Russell, *Geophys. Res. Lett.* **8**, 261 (1981).

5. T. W. Speiser, *J. Geophys. Res.* **70**, 1717 (1965).

6. V. M. Vasyliunas, *Rev. Geophys.* **13**, 303 (1965).

7. E. W. Hones, Jr., D. N. Baker, S. J. Bame, W. C. Feldman, J. T. Gosling, D. J. McComas, R. D. Zwickl, J. A. Slavin, E. J. Smith, and B. T. Tsurutani, *Geophys. Res. Lett.* **11**, 5 (1984).

8. M. Scholer, G. Gloeckler, B. Klecker, F. M. Ipavich, D. Hovestadt, and E. J. Smith, *J. Geophys. Res.* **89**, 6717 (1984).

9. E. W. Hones, Jr., J. Birn, D. N. Baker, S. J. Bame, W. C. Feldman, D. J. McComas, R. D. Zwickl, J. A. Slavin, E. J. Smith, and B. T. Tsurutani, *Geophys. Res. Lett.* **11**, 1046 (1984).

10. I. G. Richardson and S. W. H. Cowley, *J. Geophys. Res.* **90**, 12133 (1985).

FIGURE CAPTIONS

Fig. 1. Magnetic configurations of the magnetotail. A: The configuration during quiet (nonsubstorm) conditions. The dawn-to-dusk electric field is indicated as well as the equatorward $\overline{E} \times \overline{B}$ drift, $\overline{V}_E$, that it drives. The tail lobes are shown in this panel. The remaining panels show only the plasma sheet. See text for further description.

Fig. 2. Occurrence rate of fast plasma flow in the plasma sheet boundary layer and adjoining central plasma sheet. The left-most two points on each curve are central plasma sheet; the other five points are plasma sheet boundary layer. The curves with crosses are for crossings from the lobe to the central plasma sheet. The curves with circles are for crossings from the central plasma sheet to the lobe. Dashed curves are for observations from $-14\ R_E < X_{GSM} < -9\ R_E$. Dotted curves are for observations from $X_{GSM} < -14\ R_E$ (from /3/).

Fig. 3. Plasma parameters for ions at ISEE 1 (bottom three plots) and the concurrent AE index (top) on April 5, 1978. V_x is the component of the ion bulk velocity along the sun-earth line, taken positive sunward. V_{bx} is the beam velocity defined as the ion velocity corresponding to a peak in the velocity distribution. DZ_{NS} is the estimated distance of the satellite from the neutral sheet. Distances are given in earth radii (from /2/).

Fig. 4. Scatter plot of the x component of ion bulk velocity, V_x, versus ion pression (top) and a diagram showing the velocity averaged in pressure bins (bottom). All 6-second ISEE 1 data points available between 1800 and 2400 UT on April 5, 1978 with reliable velocity measurements are used in the scatter plot. The circles and error bars in the bottom panel give the bin average and standard deviation (from /2/).

Fig. 5. Features of several boundary crossings measured by ISEE 1 between 2000 UT and 2030 UT, April 5, 1978. Shown are the ion pressure, the ion flow velocity, V_x (the first moment of the ion distribution function) and, at bottom, a "gray scale" representation of $f_i(V_x)$, where the magnitude of $f_i(V_x)$ (the ion distribution function, as denoted by the subscript, i) at each velocity, V_x (each energy level of the electrostatic analyzer) is depicted by a degree of darkness (darker being higher magnitude) along a single vertical strip. Each vertical strip depicts the measurements made most nearly along the GSE +x and −x directions in one 6-second data period; thus the diagram is composed of 10 strips each minute (from /2/).

Fig. 6a. Averaged 128-second angular distributions of 75–115 keV electrons, 112–157 keV protons and 30–36 keV protons during a article burst on February 16, 1983. The earthward direction is to the left. The intensity is plotted linearly versus the instrument look direction. The number given in the sector with the highest intensity is the count rate in that sector (from /9/).

Fig. 6b. High time resolution intensity-time profiles of energetic electrons and protons for the burst on February 16, 1983 (from /9/).

Fig. 7. Schematic representation of the plasmoid passage past ISEE 3 on February 16, 1983 for which data are shown in Figures 6a and 6b. ISEE 3 crosses the separatrix layer between A and B and again after D (from /9/).

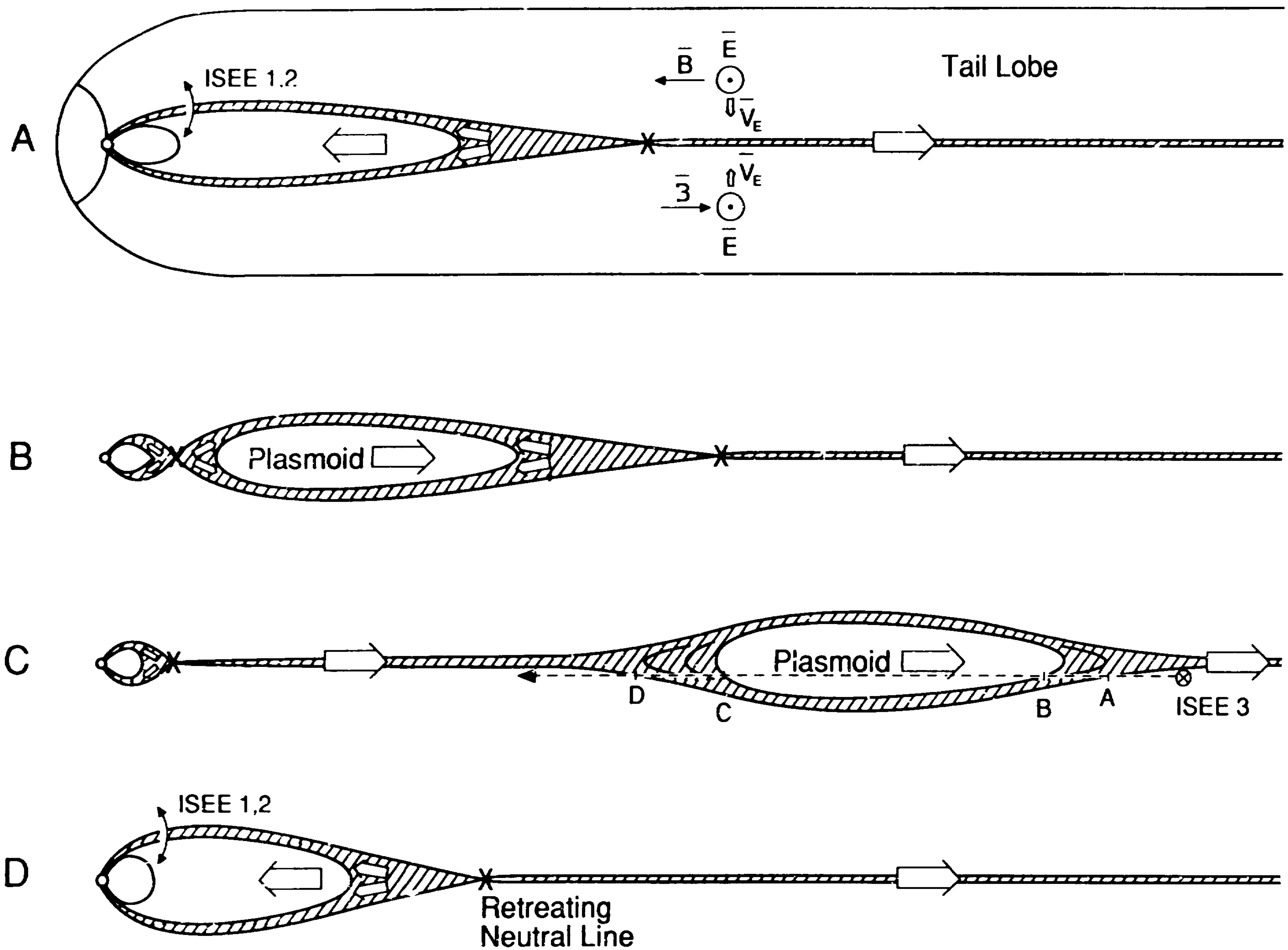
A
ISEE 1,2
B
E
V_E
3
Tail Lobe
B
Plasmoid
C
Plasmoid
D
C
B
A
ISEE 3
D
ISEE 1,2
Retreating
Neutral Line

Fig. 1

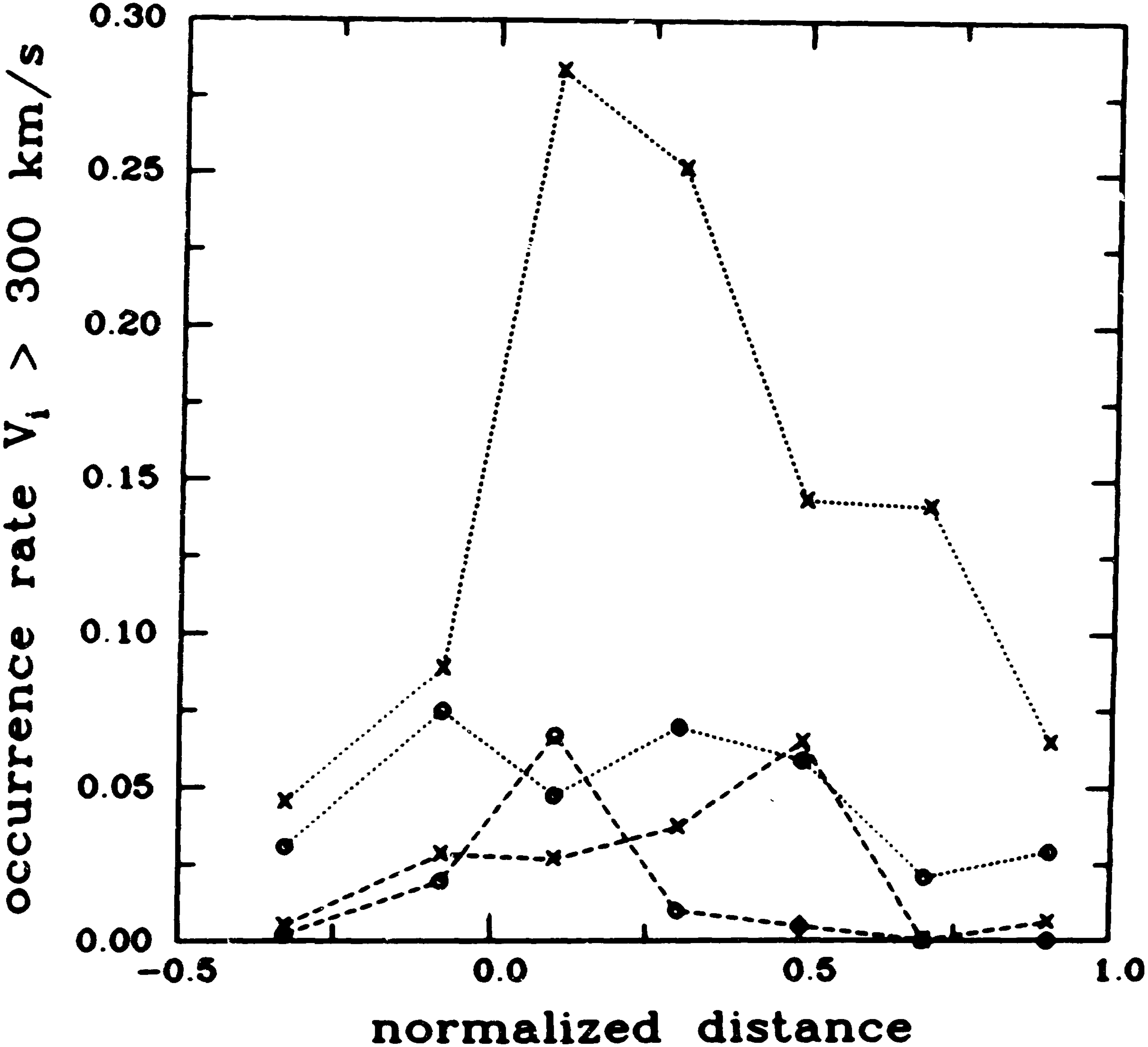

0.30
0.25
0.20
0.15
0.10
0.05
0.00
−0.5
0.0
0.5
1.0
occurrence rate V_i > 300 km/s
normalized distance

Fig. 2

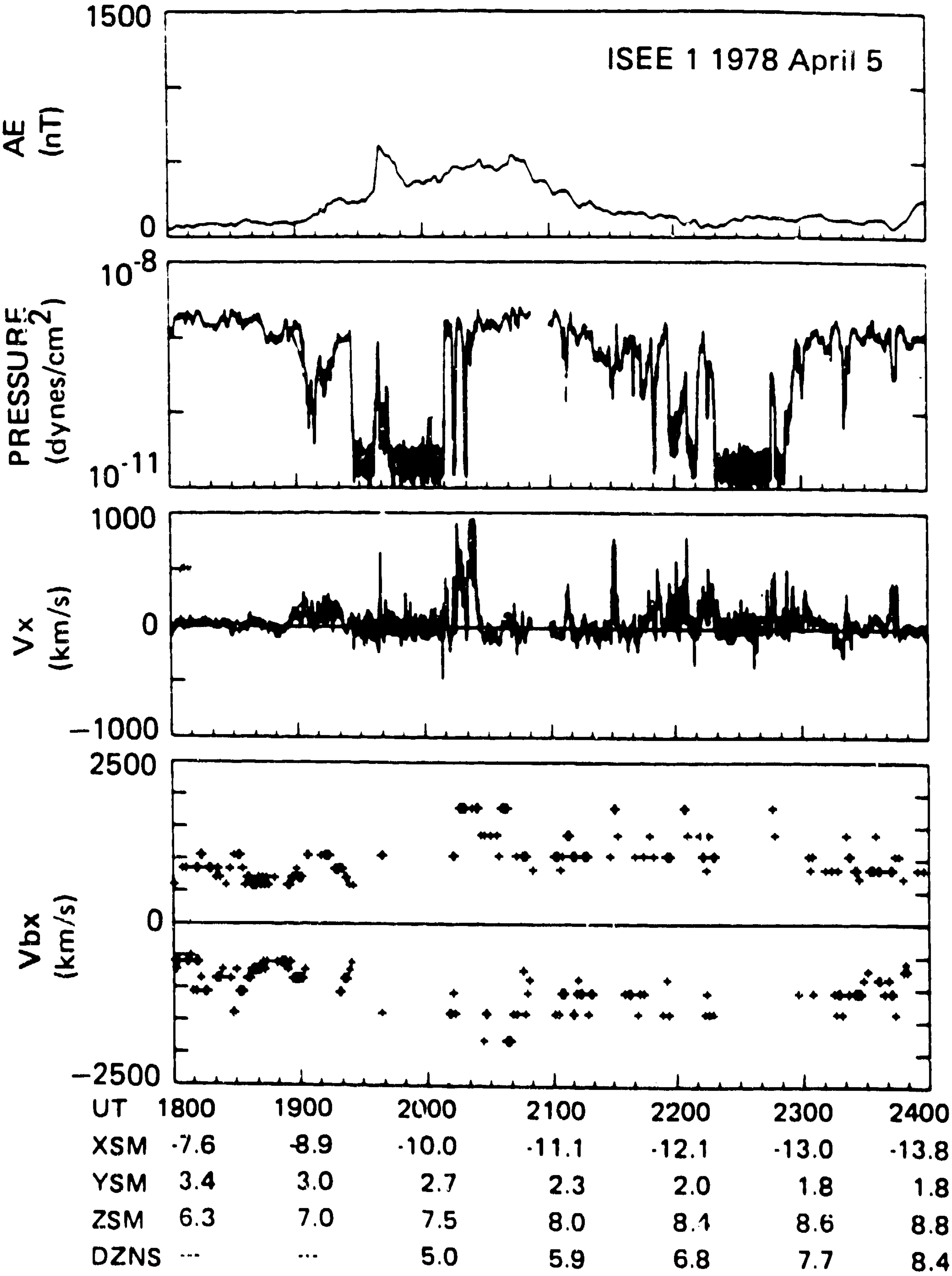

ISEE 1 1978 April 5
AE (nT)
1500
0
PRESSURE (dynes/cm^2)
10^{-8}
10^{-11}
Vx (km/s)
1000
0
−1000
Vbx (km/s)
2500
0
−2500
UT 1800 1900 2000 2100 2200 2300 2400
XSM -7.6 -8.9 -10.0 -11.1 -12.1 -13.0 -13.8
YSM 3.4 3.0 2.7 2.3 2.0 1.8 1.8
ZSM 6.3 7.0 7.5 8.0 8.4 8.6 8.8
DZNS --- --- 5.0 5.9 6.8 7.7 8.4

Fig. 3

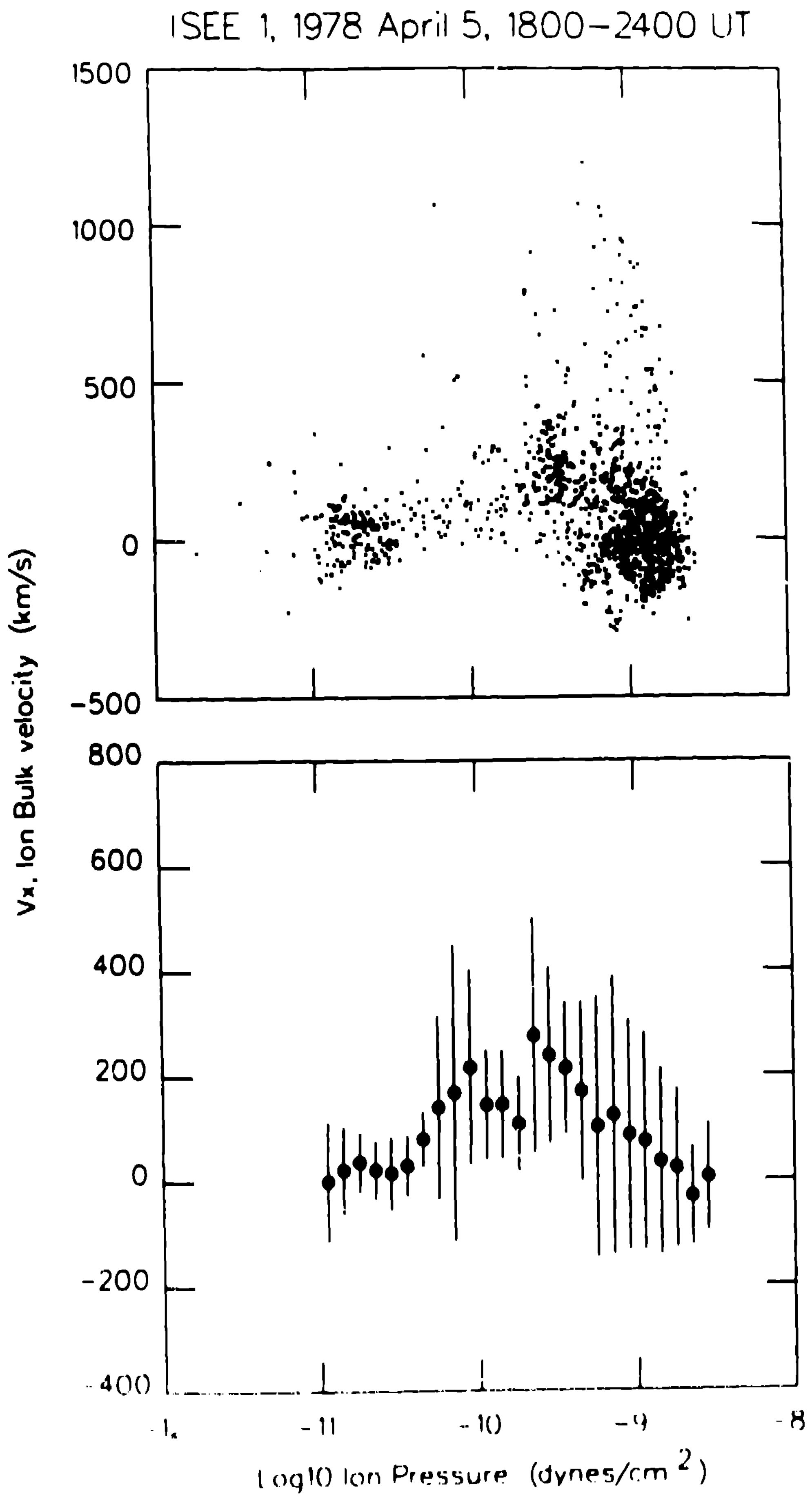
ISEE 1, 1978 April 5, 1800−2400 UT
1500
1000
500
0
−500
800
600
400
200
0
-200
-400
Vx, Ion Bulk velocity (km/s)
-11
-10
-9
-8
Log10 Ion Pressure (dynes/cm 2)

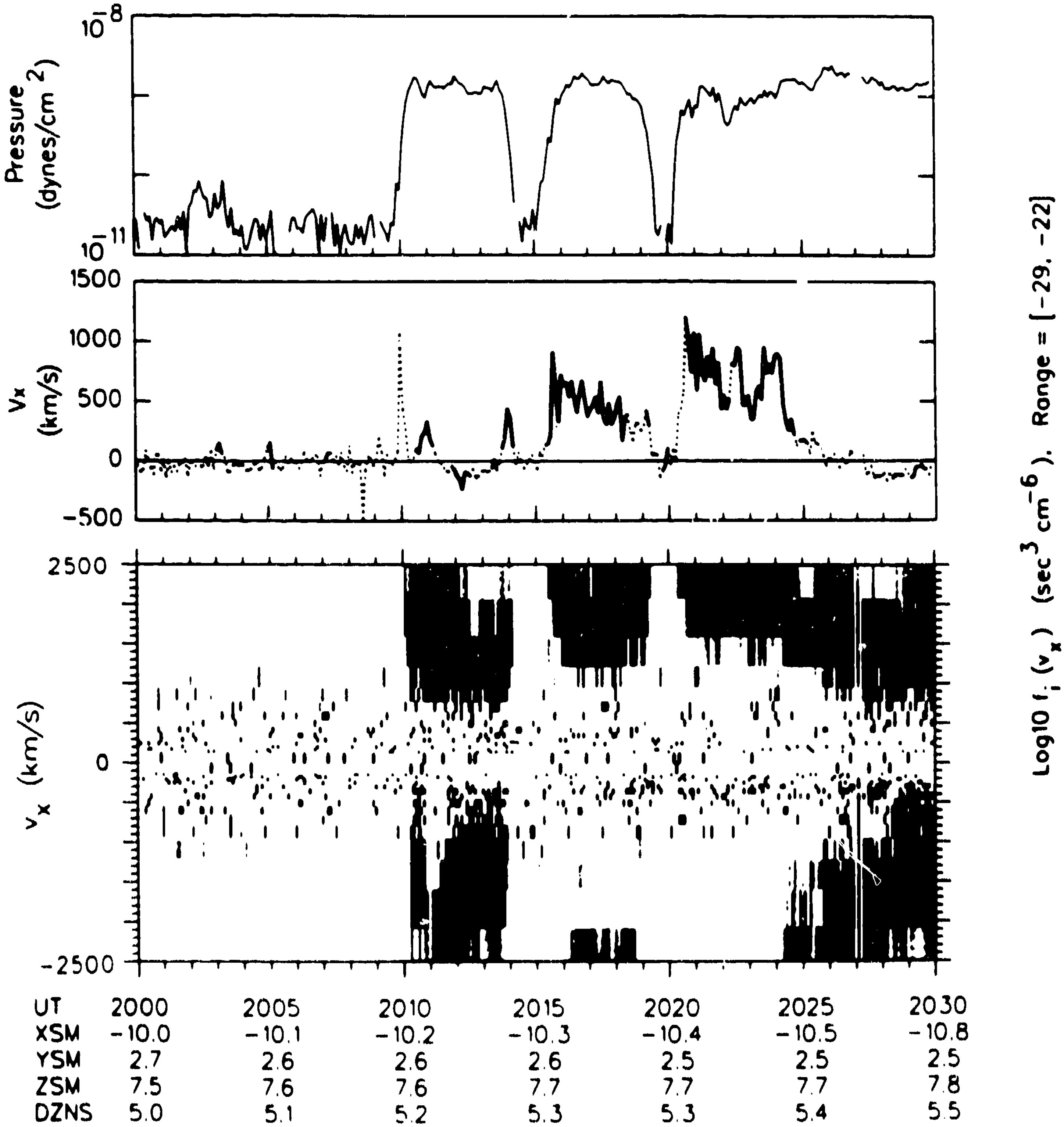
Pressure (dynes/cm 2)
10-8
10-11
Vx (km/s)
1500
1000
500
0
-500
vx (km/s)
2500
0
-2500
Log10 fi (vx) (sec3 cm-6). Range = [-29. -22]
UT 2000 2005 2010 2015 2020 2025 2030
XSM -10.0 -10.1 -10.2 -10.3 -10.4 -10.5 -10.8
YSM 2.7 2.6 2.6 2.6 2.5 2.5 2.5
ZSM 7.5 7.6 7.6 7.7 7.7 7.7 7.8
DZNS 5.0 5.1 5.2 5.3 5.3 5.4 5.5

Fig. 5

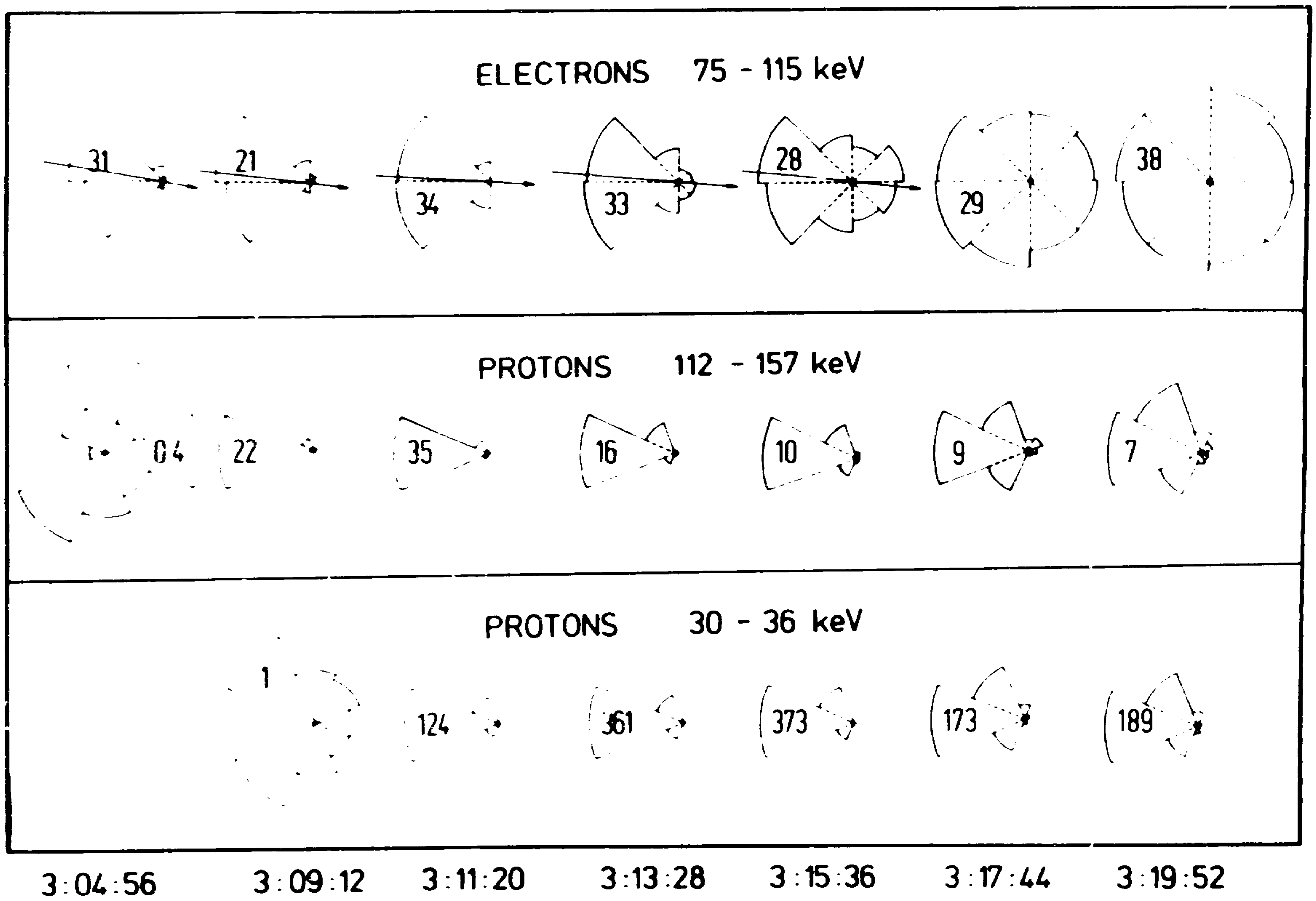
ELECTRONS 75 - 115 keV
31
21
34
33
28
29
38
PROTONS 112 - 157 keV
04
22
35
16
10
9
7
PROTONS 30 - 36 keV
1
124
361
373
173
189
3:04:56
3:09:12
3:11:20
3:13:28
3:15:36
3:17:44
3:19:52

Fig. 6a

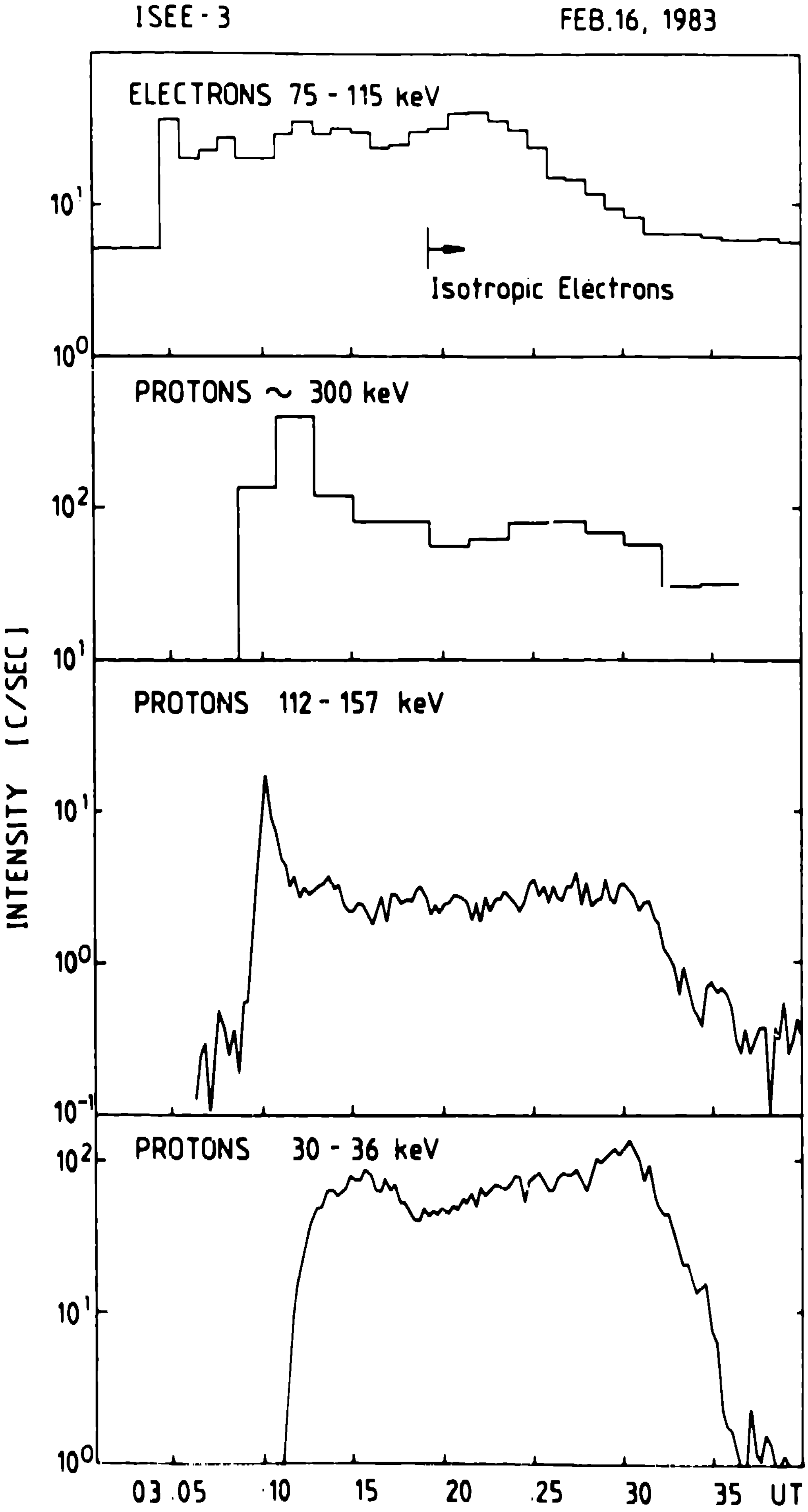
ISEE-3
FEB.16, 1983
ELECTRONS 75 - 115 keV
Isotropic Electrons
PROTONS ~ 300 keV
PROTONS 112 - 157 keV
PROTONS 30 - 36 keV
INTENSITY [C/SEC]
03 .05
10
15
20
25
30
35
UT

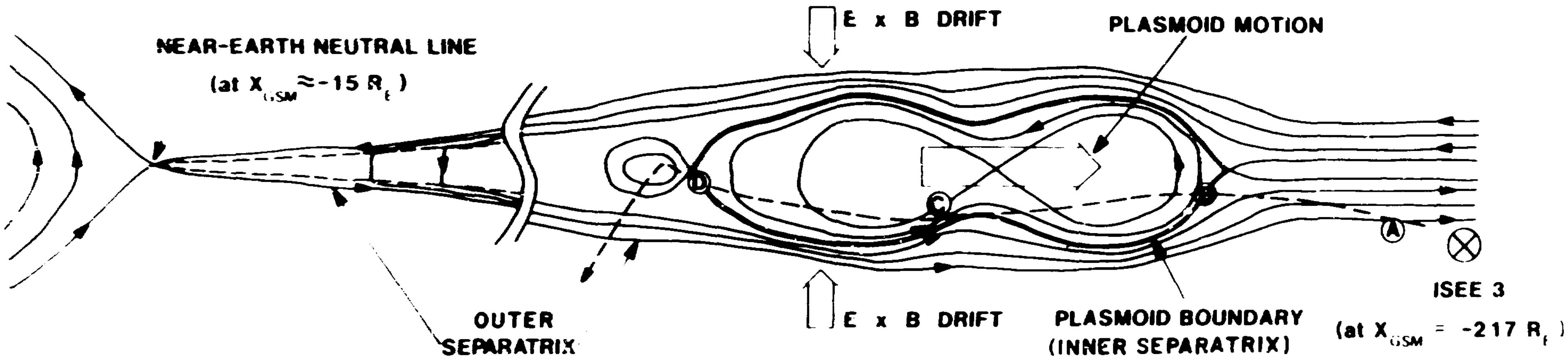
NEAR-EARTH NEUTRAL LINE
(at $X_{GSM} \approx -15\ R_E$)
E x B DRIFT
PLASMOID MOTION
OUTER
SEPARATRIX
E x B DRIFT
PLASMOID BOUNDARY
(INNER SEPARATRIX)
ISEE 3
(at $X_{GSM} = -217\ R_E$)

Fig. 7